International Journal of Nanoelectronics and Materials
Volume 16 (Special Issue) December 2023 [241-252]

Electrochemical Sensors for Detection of Glucose based on Electrochemically Reduced Graphene Oxide: Optimization of pH and Number of Cycles

Muhammad Haziq Ilias[1], Norhazlin Khairuddin[1], Maizatul Zolkapli[1], Zainiharyati Mohd Zain[2], Noor Fitrah Abu Bakar[3], Rozina Abdul Rani[4], Azrif Manut[1], and Ahmad Sabirin Zoolfakar[1,*]

[1]School of Electrical Engineering, College of Engineering, Universiti Teknologi MARA, 40450 Shah Alam, Selangor, Malaysia
[2]Faculty of Applied Sciences, Universiti Teknologi MARA, 40450 Shah Alam, Selangor, Malaysia
[3]School of Chemical Engineering, College of Engineering, Universiti Teknologi MARA, 40450 Shah Alam, Selangor, Malaysia
[4]School of Mechanical Engineering, College of Engineering, Universiti Teknologi MARA, 40450 Shah Alam, Selangor, Malaysia

ABSTRACT

Glucose determination method had gain significant interest from the industry for a fast and efficient response especially in the medical area for diabetes patient. Reduced graphene oxide (RGO) had been reported to help and improve the sensitivity of a sensor. The investigation for the optimum pH concentrations using FESEM, EDX, XRD analysis and Raman spectroscopy indicate that the pH 9 was suited to be deposited on the SPGE. In addition to that, different number of cycles during electrodeposition process was employed. Electrochemical impedance spectroscopy (EIS) was used to investigate the charge transfer resistance for each cycle. All the deposited RGO on screen-printed gold electrode (SPGE) was being compared to the bare SPGE to confirmed that the electrodeposition of RGO could decrease the charge transfer resistance. For the detection of glucose, cyclic voltammetry (CV) and differential pulse voltammetry (DPV) was used. 10 cycles deposition of RGO shows the highest sensitivity of 1.0525 $\mu A \cdot mM^{-1} \cdot cm^{-2}$ in the detection of glucose compared to the other cycles. The ease of use and scalability of the electrodeposition technique may make it easier to build upon the results of this work and produce glucose sensors that are more widely available and less expensive.

Keywords: Electrodeposition, Glucose detection, Reduced graphene oxide (RGO), Screen-printed gold electrode (SPGE)

1. INTRODUCTION

In recent years, fast and effective glucose determination methods are becoming more and more relevant in the fields of biology, chemistry, and the food business; glucose determination is crucial in the medical field for the treatment of diabetes. Diabetes is a major cause of mortality and disability and a global public health concern [1]. It is a chronic condition that arises from either insufficient insulin production by the pancreas to regulate blood sugar levels or insufficient insulin utilisation by the body. Proper diabetes management is necessary to prevent or postpone the onset of diabetic complications. It is essential to regularly check physiological blood glucose levels to ensure that medications are working and to prevent hypo- or hyperglycemia [2].

* Corresponding authors: ahmad074@uitm.edu.my

Many types of electrochemical glucose biosensors have been developed throughout the years since the first ones were developed by Clark and Lyons in 1962 [3]. Throughout the years, researchers have given the development of electrochemical biosensors a great deal of attention; as a result, the number of studies on electrochemical biosensors has risen during the past two decades. The field has been researched theoretically and practically using a variety of biosensors, including optical, thermometric, piezoelectric, magnetic, and hybrid devices that use more than one kind. This is due to the possibility of electrochemical biosensors to offer an alluring solution for bulky and expensive analytical instruments [4].

One factor that affects the redox reaction rate in an electrochemical cell for an electrochemical biosensor is the electrode's catalytic activity. A highly catalytic electrode amplifies the redox reaction and hence the signal (current) [5]. Increasing electron transport processes and improving the ability of active materials to bind to the electrode are two major effects of using graphene as an electrode material [3]. Pure graphene has exceptional physical, chemical, mechanical, electrical, and thermal properties, but because of its high cost and inability to scale up industrially, it is rarely used in the creation of biosensors [6]. This is because of strong π - π stacking or van der Waals interactions between individual graphene sheets, which lead graphene to permanently agglomerate and precipitate in aqueous solutions [7], [8], [9], which results in limitations such low water dispersibility, difficult production processes, and a reduction in active surface sites from aggregation, which might reduce sensor activity [10], [11] and limit its application in biosensor. These challenges are partially mitigated by the use of chemically modified oxygenated graphene derivatives, such as reduced graphene oxide (RGO), which is decorated with functionalities including epoxy, carbonyl, carboxyl, and hydroxyl. It possesses enhanced graphene oxide (GO) characteristics, such as the ability to modify the number of oxygen groups, in addition to strong mechanical and conductive capabilities akin to graphene [10], [12]. The electrodeposition approach is one of the most appealing RGO preparation processes because of its economical and environmentally favourable characteristics. According to the findings, RGO that exhibited a single sheet-like nature chemically demonstrated good electrochemical activity [13].

The aim of this study was to investigate the optimum pH concentrations to the formation of RGO on the screen-printed gold electrode (SPGE) as a sensing membrane. The importance in finding the optimum pH concentration is to confirm that the deposition of RGO on SPGE is more uniform and could improve electrical conductivity of the sensor. The optimum pH concentration was being chosen from the characterization of RGO and being deposited in different number of cycles on SPGE for glucose detection. The optimum pH concentration and number of cycles of electrodeposition of RGO was expected to improve the electrodeposition of RGO on SPGE.

2. MATERIAL AND METHODS

2.1 Materials and Reagents

Graphene Oxide (GO) powder was purchased from GO Advanced Solution. Phosphate Buffer Saline was from R&M Chemicals for both pH7 and pH7.4, while sodium hydroxide (NaOH) granules and D-glucose was purchased from Sigma Aldrich.

2.2 Apparatus and Measurements

All of the fabrication was carried out with Metrohm Autolab's Autolab PGSTAT204. A field emission scanning electron microscope (FESEM) was used to examine the surface morphology of RGO. An investigation of RGO's elemental composition was conducted using energy dispersive X-ray (EDX) methodology. The crystalline structure of the RGO was investigated using X-ray diffraction (XRD) analysis, and the chemical composition and structure of the RGO on SPGE were investigated using RAMAN spectroscopy. PalmSens4 was used for all electrochemical tests of cyclic voltammetry (CV) and different pulse voltammetry (DPV).

2.3 Preparation of Graphene Oxide (GO) Solution

Sodium hydroxide granules were added to 300mL of phosphate buffer saline (PBS) in order to alter the pH until the required pH was reached. To create multiple pH of graphene oxide (GO) solution, the pH of the PBS was altered from pH 8, pH 9, and pH 10. The pH concentration was chosen from pH 8 to pH 10 was because the GO solution had excellent aqueous dispersions in higher pH concentrations [14]. Once the desired pH was obtained, 0.15g of GO powder was added, combined with the PBS solution, and stirred for 15 minutes at room temperature.

2.4 Electrodeposition of RGO on SPGE

Reduced graphene oxide (RGO) was synthesised on screen-printed gold electrodes (SPGE) using the method of the electrodeposition. The working electrode was made of gold, while the counter and reference electrodes were made of platinum and silver, respectively. Before starting the electrodeposition process, the glass vessel holding the GO solution was immersed in a water bath at 40°C to attain equilibrium temperature. Cyclic voltammetry (CV) was used to deposit and decrease the graphene oxide solution on the SPGE. Each window parameter was assessed at -0.85V (start-stop potential), and the voltammetry window parameters utilised were -0.85V to -1.5V sweep potential (lower and upper vertex) at 0.005 V/s scan rate.

3. RESULTS AND DISCUSSION

3.1 Surface Morphology of RGO

The microstructures of RGO with varied pH concentration were investigated with FESEM. The pH concentration was varied from pH8 to pH10. The concentration of pH was adjusted between pH 8 and pH 10. The production of RGO on the SPGE is validated by the FESEM picture (Figure 1), which shows that the surface was rough and wrinkled due to RGO synthesis. This might be explained by the fact that when the electrode potential dropped to a negative value during electrodeposition, GO was electrochemically reduced to produce RGO, which is very hydrophobic [15]. From the images, the effect of pH concentration can be observed on how the RGO formed on the surface of SPGE. The RGO for pH8 shows that the RGO is not stacked and partially folded. The pH 9 was stacked uniformly and a slight fluctuation was observed. Moving to pH 10, the RGO starts to agglomerate however the amount of wrinkles increase.

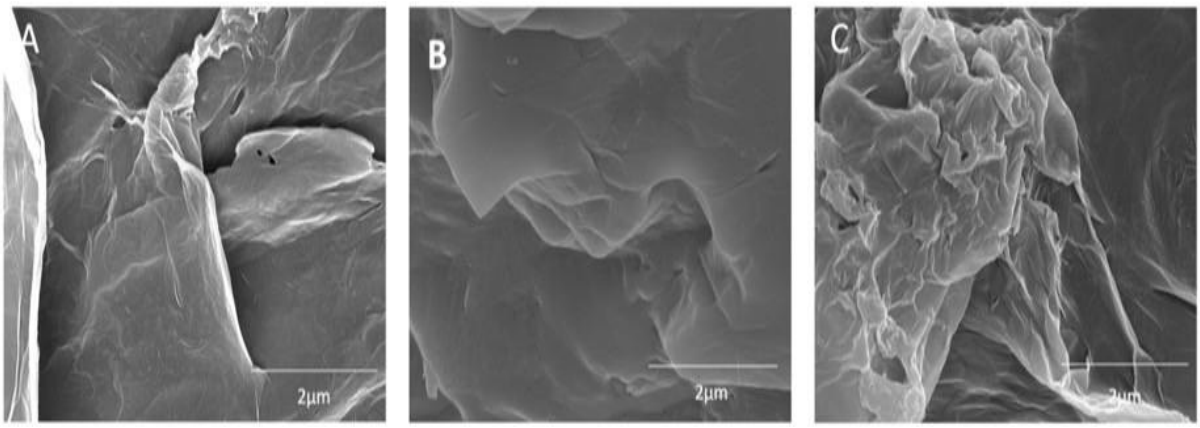

Figure 1. FESEM image of RGO for different pH: A) pH8 B) pH9 C) pH10.

Table 1 EDX analysis of RGO with different pH concentration

	Carbon (C)		Oxygen (O)		Totals (/100%)	
	Weight %	**Atomic %**	**Weight %**	**Atomic %**	**Weight%**	**Atomic%**
pH 8	16.53	36.51	23.16	38.39	39.69	76.9
pH 9	39.63	49.31	44.31	41.73	83.94	91.04
pH 10	33.48	44.89	38.11	38.35	71.59	83.24

The EDX analysis of the RGO chemical composition for different pH concentration was summarised in Table 1. The weight and atomic percentage of carbon and oxygen were shown by the EDX analysis, which validates the production of RGO on the SPGE surface following the electrodeposition procedure. The overall weight and atomic percentage were not100%, indicating that impurities were present throughout the reduction process. The carbon and oxygen content for pH 8 were 36.51 at% and 38.39 at% respectively. As the pH concentrations increase to pH 9, the atomic percentage of carbon and oxygen rise to 49.31 at% and 41.73 at%. However, as the pH concentration reached to pH 10, both the carbon and oxygen atomic percentage decrease to 44.89 at% and 38.35% respectively. The possibility of the RGO interacting with other species in solution increases as the pH rises because more oxygenous functional groups on the surface of GO sheets deprotonate. This is because the RGO surface's reactivity is increased by the deprotonation of acidic functional groups [16]. As opposed to pH 8 and pH10, pH 9 had the largest atomic percentage of carbon and oxygen, indicating a lesser chance that contaminants may interfere with the sensor's detecting process.

3.2 XRD Analysis

X-ray diffraction (XRD) examination was utilised to further study the structure of RGO with varying pH concentrations. The peaks found from the XRD are shown in Figure 2. The corresponding d-spacing calculated by Bragg's law (1) and crystallite size have been reported in Table 2. The crystallite size has been determined by Scherrer's equation (2) [17]. The disorder in the graphene sheets causes the RGO diffraction peak, which is identified by the prominent peak [002] at $2\theta = 25°$ and emerges between 24° and 26°. Moreover, the absence of the graphene oxide's [001] diffraction peaks suggests that, following the chemical reduction process, the majority of the oxygen functional groups have been eliminated from the GO surface [18]. Every sample had an interlayer spacing of around 0.34 nm, which is consistent with what has been reported in the literature. This is because the functional group containing oxygen has been removed, indicating that the sp2 network has been restored upon reduction [19]. Furthermore, when the pH concentration increases, the intensity of the RGO peak decreases, with pH 9 having

the lowest intensity when compared to the others. Additionally, it was observed that, when pH increased, the crystalline size decreased because of the increased charge density [20]. There were four diffraction peaks at 38°, 44°, 64° and 77°, related to planes (111), (200), (220) and (311) which were assumed to be due to the surface of the SPGE which is gold. Other miscellaneous peaks are considered as the residual intercalation compounds.

$$d = \frac{\lambda}{\beta sin\theta} \tag{1}$$

$$D = \frac{k\lambda}{\beta cos\theta} \tag{2}$$

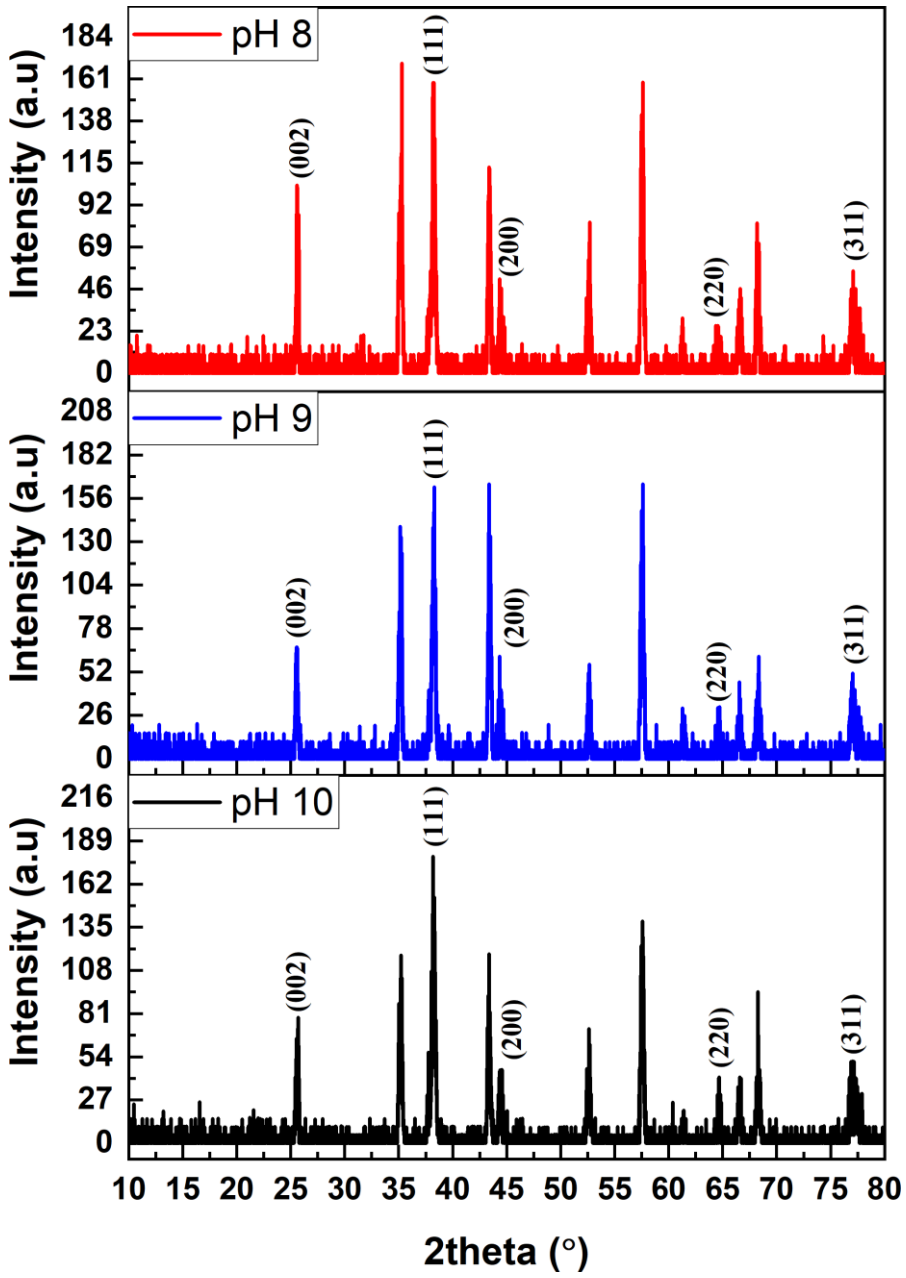

Figure 2. XRD patterns of the reduced graphene oxide (RGO) composite for pH 8, pH 9, pH 10.

Table 2 Crystallite size and interlayer spacing of RGO obtained by XRD analysis

RGO/SPGE Sample	20 (°)	d (Å)	FWHM (°)	Crystalline size (nm)
pH 8	25.611	3.4754	0.24026	35.44
pH 9	25.555	3.4829	0.25987	32.76
pH 10	25.602	3.4766	0.30654	27.78

3.3 Raman Spectroscopy

The structural changes in RGO may be understood through analysing the variations in the attributes of the D and G peaks acquired by Raman spectroscopy. Figure 3 shows the Raman spectra of the RGO/SPGE for different pH concentrations. The spectra show two distinct peaks: the D peak, located at around 1370 cm^{-1}, and the G peak, located at approximately 1580 cm^{-1}. The graphene's lattice distortion from different functional groups and defects is measured by the D peak, while the first order scattering of the E2g phonon from the sp^2 hybridised carbon lattice is measured by the G peak. Because there are more small-sized sp^2 domains following reductions, the average size of the sp^2 domain decreases, resulting in a D peak that is larger than the G peak.[21].

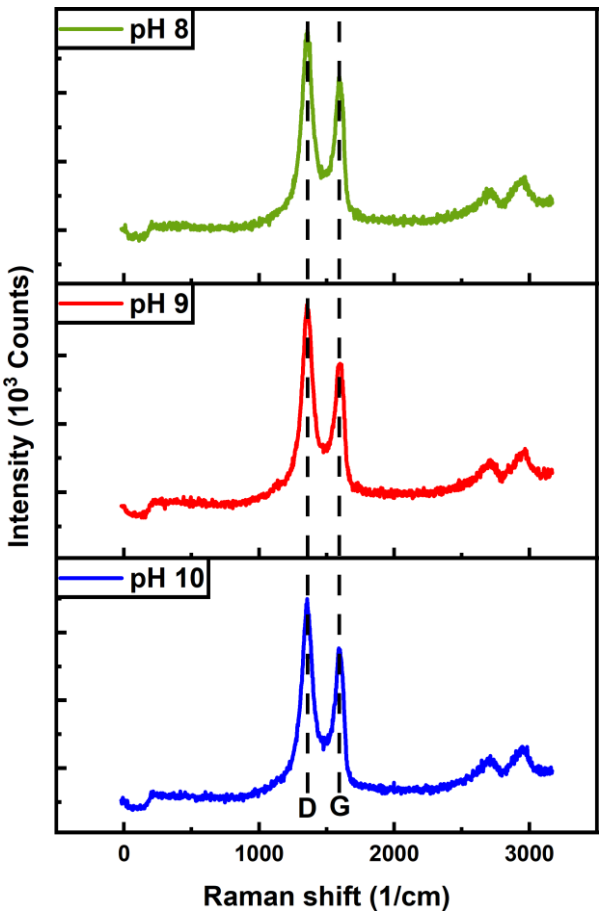

Figure 3. Raman spectra of RGO/SPGE difference in pH concentrations.

Table 3 Intensity Ratio (ID/IG) for different pH concentrations

RGO/SPGE Sample	pH 8	pH 9	pH 10
I_D/I_G	1.85	1.83	1.82

The average size of the sp^2 domains is inversely related to the intensity ratio (ID/IG) of the D and G bands, which measures the defects generated in the sample. A summary of the ID/IG ratios is reported in Table 3. Based on the table, the I_D/I_G ratio of the RGO are similar to other report on RGO [22], [23]. Due to unpaired defects in the graphite lattice caused by the loss of certain oxygen groups, the intensity ratios for the RGO also increase as the pH of the solution decrease. [24]. This is due to the fact that when the pH rises, the carboxylic groups at the edges of RGO sheets become deprotonated and charged, resulting in electrostatic repulsions between RGO sheets and the well-dispersed RGO solution [21].

3.4 Electrochemical Properties of RGO

The electrochemical property of RGO on SPGE was analysed using cyclic voltammetry (CV) and electrochemical impedance spectroscopy (EIS) experiments, with $K_4[Fe(CN)_6]$ serving as the electrochemical probe. Based on the characterization results, pH 9 shows the best conditions to be deposit on the SPGE. The CV curves for bare SPGE and RGO/SPGE with varying cycles of 5, 7, 10, and 15 are shown in Figure 4(A) at a scan rate of 0.1 V/s. The solution contains 5mM of $[Fe(CN)_6]^{3-/4-,}$ and the two peaks are similar and symmetric in nature. These peaks are related to the formation of modified electrodes' oxidation and reduction responses to the $[Fe(CN)_6]^{3-/4-}$ solution. At 0.34 V and 0.01 V, respectively, the oxidation and reduction peaks of bare SPGE were visible. Additionally, compared to the other samples, 10 cycle RGO/SPGE showed smaller peak-to-peak separation and greater current because the reduction peak emerged at 0.06 V and the oxidation peak at 0.27 V. Furthermore, as the number of cycles increases, so does the peak current and peak to peak separation, but as the number of cycles increases, both peak current and peak to peak separation drop. The results indicate that the redox process is enhanced by the electrodeposition of RGO with 10 cycles, as seen by the electrodes with the highest peak current and peak to peak separation (PGE/RGO/SPGE) when compared to the other electrodes.

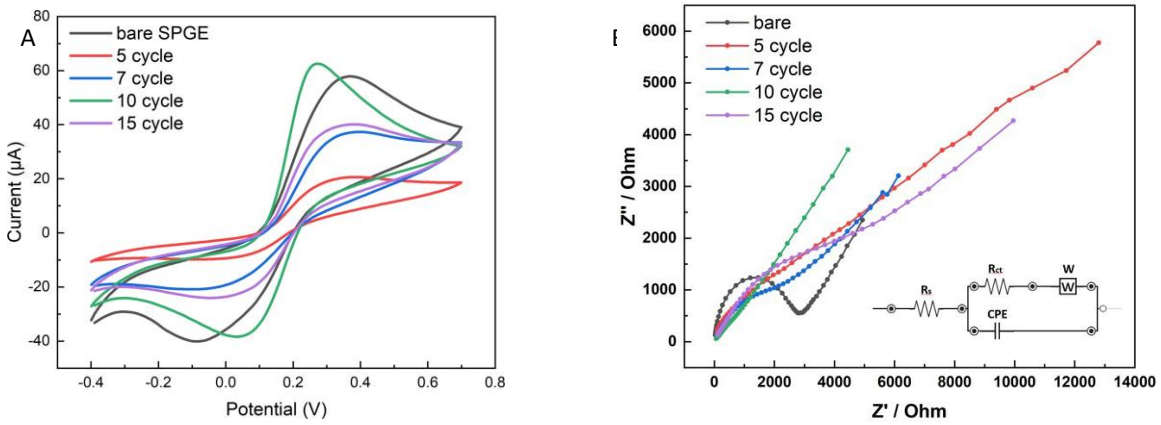

Figure 4. (A) Cyclic Voltammetry (CV) curve of bare SPGE and RGO/SPGE prepared at different number of cycles in 5mM $Fe(CN)_6^{-3/-4}$ in 0.1M KCl solution (scan rate = 0.1 V/s) and (B) nyquist plot forelectrochemical impedance spectroscopy (EIS) for bare SPGE and RGO/SPGE with different number of cycles.

Table 4 Parameters for EIS measurement obtained from fitting of nyquist plot

RGO/SPGE Sample	Rs (Θ)	Rct (Θ)	CDL	Warburg (W)
Bare	29.63	2487	6.32E-07	1941
5 cycles	118.1	1511	5.43E-07	8523
7 cycles	108.4	1153	1.39E-06	4101
10 cycles	50.71	157.4	1.663E-06	3377
15 cycles	150.6	1359	1.31E-06	6245

In order to get a deeper understanding of the features of the sensor architecture and to explain the electron transfers across each sample, the electrochemical properties of the RGO with various cycles were further investigated using electrochemical impedance spectroscopy (EIS). Vertical lines in the lower frequency range show how each electrode's capacitive behaviour is at its best. The higher frequency intercept relates to the electrode's ionic and electrical conductivity. The ions thus have a harder time passing through the electrode. This is the same as the load transfer resistance (R_{ct}) and represents the rapid rate of electron transport at the electrolyte/electrode contact [25]. The EIS was performed at open circuit potential and frequency range of 0.1 Hz – 2 kHz at bare SPGE, 5, 7, 10, and 15 cycles of RGO/SPGE in 0.1 KCl solution containing 5mM of $[Fe(CN)_6]^{3-/4-}$. The Nyquist plots of EIS obtained at the corresponding open circuit potential of the modified electrode are displayed in Figure 4(A). The restricted diffusion process is shown by the linear segment in the Nyquist plot at lower frequencies, while the restricted electron transfer process is represented by the semicircle at higher frequencies. The equivalent circuit with the electrolyte solution resistance (R_s), electron

and charge transfer resistance (R_{ct}), Warburg element (W), and constant phase element (CPE1) might match the EIS design. It is depicted in Figure 4(B) (bottom right inset). R_{ct} was controlled by the dielectric and insulating properties at the electrode-electrolyte interface.[26]. The value obtained from the Nyquist plot and the equivalent circuit is shown in Table 4. The electrodeposition of RGO had reduced the R_{ct} value of the electrode which shows that the RGO had increase the electron transfer process on the SPGE. In addition, the 10 cycles RGO/SPGE shows the lowest R_{ct} value compared to the rest of number of cycles which shows that the 10 cycles RGO/SPGE which indicate the fast electron transfer of the electrode. This is caused by enhanced electrical characteristics and the successful removal of oxygen-containing groups that are electrochemically unstable during reduction, which produces the behaviour of pseudo-capacitance. The numerous layers of RGO and therefore larger thickness resulted in improved insulating characteristics and inhibited electrochemical properties. When the number of cycles was raised by more than 10 cycles, the R_{ct} value rose.[27].

3.5 Performance of RGO/SPGE in Glucose Detection

The electrochemical performance of RGO/SPGE for glucose detection was assessed using cyclic voltammetry (CV) measurement. Figure 5 present the CV curves of bare SPGE and different cycles of RGO/SPGE with the absence and presence of glucose. The CV measurement was performed with 5mM of glucose in PBS (pH 7.0) at the scan rate of 0.1 V/s. In the absence of glucose shown in Figure 5 (A), only 10 cycles show higher current density when compared to the bare SPGE suggesting that only 10 cycles RGO/SPGE had a significant increase surface area of the SPGE which was due to the large surface area of RGO. Meanwhile, in the presence of 5mM glucose concentration which shown in Figure 5 (B), the oxidation peak reduced significantly, while the reduction peak increases. Every electrode's peak potential rises and moves further in the direction of negative values. An increased electrocatalytic activity for the oxidation of glucose is shown by the rise in the reduction peak and the clearly negative-shifted onset potential [28].

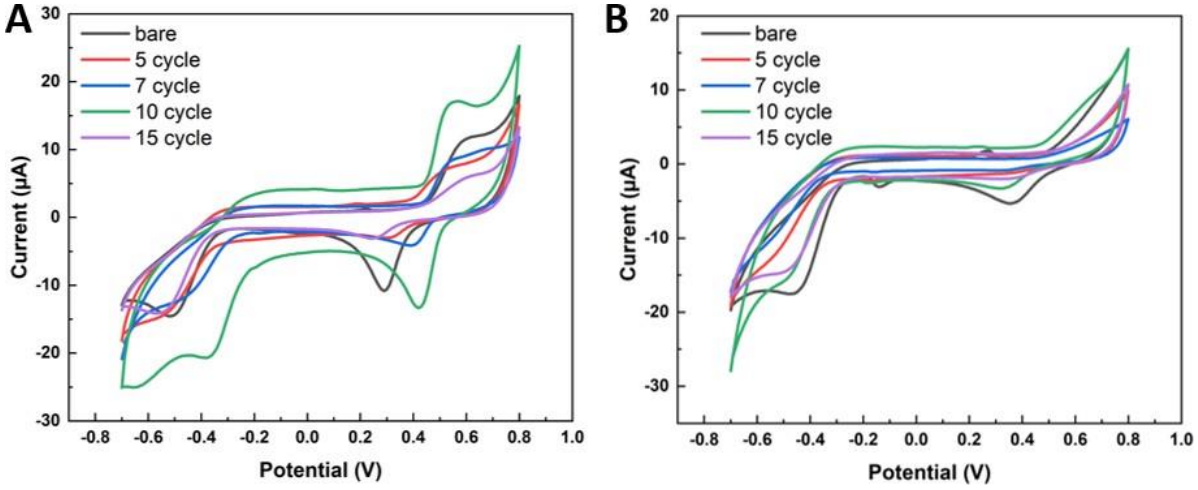

Figure 5. Comparison of bare SPGE and RGO/SPGE with and without the presence of glucose.

CV measurements with varying concentrations of glucose in PBS (pH 7.0) were also used to investigate the sensing response of RGO/SPGE. According to the CV curves shown in Figure 6 (A) of 10 cycles RGO/SPGE, when glucose concentration increased, the reduction current dropped. The creation of a sensitive biosensor depends on how the electrode responds to a decrease in reduction current.

Using differential pulse voltammetry (DPV), the calibration plot was obtained. Figure 6 (B) displays the DPV responses of 10 cycles of RGO/SPGE at various glucose concentrations in PBS (pH 7.0). The cathodic peak decreased as glucose content increased, although the curves showed a clearly defined peak reduction peak between potentials of -0.4V and -0.5V. Table 5 displays the data obtained for the other cycle, and Figure 6 (C) displays the calibration curve produced from the DPV graph of 10 cycles RGO/SPGE between the cathodic peak current and the concentration of glucose in the range of 0 mM to 10 mM. The correlation coefficient for 10 cycles RGO/SPGE is R^2 = 0.961. The sensitivity of 1.0525 $\mu A \cdot mM^{-1} \cdot cm^{-2}$ was calculated from the slope of the calibration plot. Table 5 shows the correlation coefficient (R^2), and sensitivity for each cycle of RGO/SPGE. The 10 cycles RGO/SPGE had the highest sensitivity when compared to the other cycles. It can be observed that the sensitivity increases when the number of cycles increase. However, the sensitivity starts to drop as the number of cycles increases further. The sensitivity value of 10 cycles was agreed with the EIS results which stated that the 10 cycles RGO/SPGE had the lowest charge transfer resistance which affecting the sensitivity and conductivity of the sensor in glucose detection.

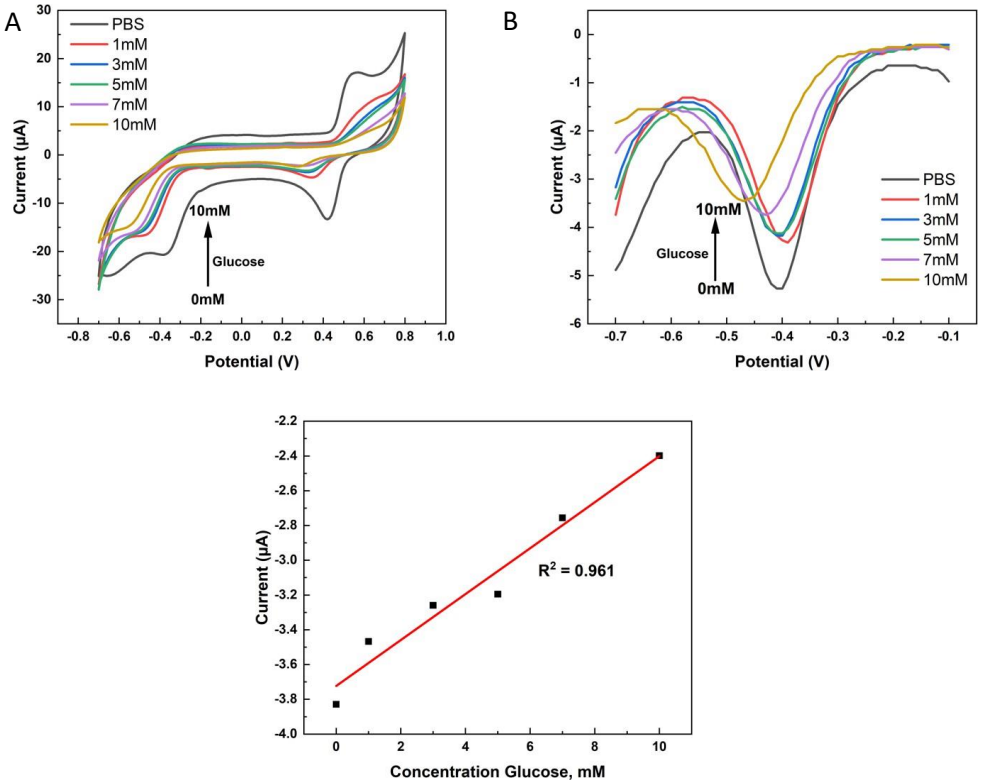

Figure 6. (A) CV for different glucose concentrations. (B) DPV for different concentrations (C) Calibration plot obtained from the DPV.

Table 5 Sensitivity for each cycle obtained from calibration plot

Number of Cycles	Correlation Coefficient (R^2)	Sensitivity ($\mu A \cdot mM^{-1} \cdot cm^{-2}$)
5	0.9829	0.4984
7	0.9263	0.9562
10	0.961	1.0525
15	0.9051	0.7476

4. CONCLUSION

The reduced graphene oxide (RGO) was deposited on the screen-printed gold electrode (SPGE) using electrodeposition method. The characterization using Field Emission Scanning Electron Microscopy (FESEM), EDX, XRD analysis and Raman spectroscopy indicates that the optimum pH concentrations of RGO was pH 9. The optimum pH was used in the fabrication of RGO/SPGE for different cycles during the electrodeposition process. The number of cycles was varied to 5, 7, 10 and 15 cycles. The number of cycles prove that the RGO was best at 10 cycles as the surface area of the increase as well as the sensitivity of the sensor.

ACKNOWLEDGEMENTS

The authors gratefully appreciated the support of the Fundamental Research Grant Scheme (FRGS) with grant number is 600-RMC/FRGS 5/3 (082/2023) by Ministry of Higher Education Malaysia.

REFERENCES

[1] H. Liu, C. A. Tao, Z. Hu, S. Zhang, J. Wang, & Y. Zhan, "An electrochemical glucose biosensor based on graphene composites: Use of dopamine as reducing monomer and as site for covalent immobilization of enzyme," RSC Adv, vol. 4, no. 82, pp. 43624–43629, 2014.

[2] N. Mohamad Nor, N. S. Ridhuan, & K. Abdul Razak, "Progress of Enzymatic and Non-Enzymatic Electrochemical Glucose Biosensor Based on Nanomaterial-Modified Electrode," Biosensors, vol. 12, no. 12. MDPI, Dec. 01, 2022.

[3] C. Wang *et al*., "Ag–Pt hollow nanoparticles anchored reduced graphene oxide composites for non-enzymatic glucose biosensor," Journal of Materials Science: Materials in Electronics, vol. 27, no. 9, pp. 9370–9378, Sep. 2016.

[4] H. A. Abdulbari & E. A. M. Basheer, "Electrochemical Biosensors: Electrode Development, Materials, Design, and Fabrication," ChemBioEng Reviews, vol. 4, no. 2. Wiley-Blackwell, pp. 92–105, 2017.

[5] C. Y. Chan *et al*., "A reduced graphene oxide-Au based electrochemical biosensor for ultrasensitive detection of enzymatic activity of botulinum neurotoxin A," Sens Actuators B Chem, vol. 220, pp. 131–137, Jun. 2015.

[6] A. Popov *et al*., "Reduced graphene oxide and polyaniline nanofibers nanocomposite for the development of an amperometric glucose biosensor," Sensors (Switzerland), vol. 21, no. 3, pp. 1–15, Feb. 2021.

[7] S. Hu *et al*., "Reduced graphene oxide-carbon dots composite as an enhanced material for electrochemical determination of dopamine," Electrochim Acta, vol. 130, pp. 805–809, Jun. 2014.

[8] N. Khairudin *et al*., "Enhancing Humidity Performance: Effect of Electrode Material on Electrochemical Reduced Graphene Oxide (ERGO) Humidity Sensor," International Journal of Integrated Engineering, vol. 14, no. 3, pp. 215–228, 2022.

[9] M. H. Ilias *et al*., "Effect of interdigital electrode material on the performance of an electrochemically Reduced Graphene Oxide chemiresistive humidity sensor," in Proceedings - 2021 IEEE Regional Symposium on Micro and Nanoelectronics, RSM 2021, Institute of Electrical and Electronics Engineers Inc., Aug. 2021, pp. 133–136.

[10] D. Chauhan, Pooja, V. Nirbhaya, C. M. Srivastava, R. Chandra, & S. Kumar, "Nanostructured transition metal chalcogenide embedded on reduced graphene oxide based highly efficient biosensor for cardiovascular disease detection," Microchemical Journal, vol. 155, Jun. 2020.

[11] N. Khairudin *et al*., "Effect of IDE Spacing on the Performance of ErGO Chemiresistive Humidity Sensor," in Proceedings - 2021 IEEE Regional Symposium on Micro and Nanoelectronics, RSM 2021, Institute of Electrical and Electronics Engineers Inc., Aug. 2021, pp. 108–111.

[12] N. S. Khairir *et al*., "Schottky behavior of reduced graphene oxide at various operating temperatures," Surfaces and Interfaces, vol. 6, pp. 229–236, Mar. 2017.

[13] S. Li, J. X. Xiong, C. X. Chen, F. Q. Chu, Y. Kong, & L. H. Deng, "Amperometric biosensor based on electrochemically reduced graphene oxide/poly(m-dihydroxybenzene) composites for glucose determination," Materials Technology, vol. 32, no. 1, pp. 1–6, Jan. 2017.

[14] S. Kashyap, S. Mishra, & S. K. Behera, "Aqueous Colloidal Stability of Graphene Oxide and Chemically Converted Graphene," Journal of Nanoparticles, vol. 2014, pp. 1–6, Nov. 2014.

[15] P. Moozarm Nia, W. P. Meng, F. Lorestani, M. R. Mahmoudian, & Y. Alias, "Electrodeposition of copper oxide/polypyrrole/reduced graphene oxide as a nonenzymatic glucose biosensor," Sens Actuators B Chem, vol. 209, pp. 100–108, Mar. 2015.

[16] W. Peng, H. Li, Y. Liu, & S. Song, "A review on heavy metal ions adsorption from water by graphene oxide and its composites," Journal of Molecular Liquids, vol. 230. Elsevier B.V., pp. 496–504, Mar. 01, 2017.

[17] F. Yusoff & K. Suresh, "Performance of reduced graphene oxide/iron(III) oxide/silica dioxide (rGO/Fe3O4/SiO2) as a potential oxygen reduction electrocatalyst in fuel cell," Sains Malays, vol. 50, no. 7, pp. 2017–2024, Jul. 2021.

[18] Y. Zhang, J. Liu, Y. Zhang, J. Liu, & Y. Duan, "Facile synthesis of hierarchical nanocomposites of aligned polyaniline nanorods on reduced graphene oxide nanosheets for microwave absorbing materials," RSC Adv, vol. 7, no. 85, pp. 54031–54038, 2017.

[19] V. Sharma, Y. Jain, M. Kumari, R. Gupta, S. K. Sharma, & K. Sachdev, "Synthesis and Characterization of Graphene Oxide (GO) and Reduced Graphene Oxide (rGO) for Gas Sensing Application," Macromol Symp, vol. 376, no. 1, Dec. 2017.

[20] X. Hu, Y. Yu, W. Hou, J. Zhou, & L. Song, "Effects of particle size and pH value on the hydrophilicity of graphene oxide," Appl Surf Sci, vol. 273, pp. 118–121, May 2013.

[21] Y. E. Shin *et al*., "An ice-templated, pH-tunable self-assembly route to hierarchically porous graphene nanoscroll networks," Nanoscale, vol. 6, no. 16, pp. 9734–9741, Aug. 2014.

[22] S. Fang *et al*., "Three-dimensional reduced graphene oxide powder for efficient microwave absorption in the S-band (2-4 GHz)," RSC Adv, vol. 7, no. 41, pp. 25773–25779, 2017.

[23] A. D. Smith *et al*., "Toward CMOS compatible wafer-scale fabrication of carbon-based microsupercapacitors for IoT," in Journal of Physics: Conference Series, Institute of Physics Publishing, Jul. 2018.

[24] D. E. Glass & G. K. Surya Prakash, "Effect of pH on the Reduction of Graphene Oxide on its Structure and Oxygen Reduction Capabilities in the Alkaline Media," Electroanalysis, vol. 30, no. 9, pp. 1938–1945, Sep. 2018.

[25] A. R. Marlinda *et al*., "Gold nanorods-coated reduced graphene oxide as a modified electrode for the electrochemical sensory detection of NADH," J Alloys Compd, vol. 847, Dec. 2020.

[26] J. Chen *et al*., "A highly sensitive amperometric glutamate oxidase microbiosensor based on a reduced graphene oxide/prussian blue nanocube/gold nanoparticle composite film-modified pt electrode," Sensors (Switzerland), vol. 20, no. 10, May 2020.

[27] P. Moozarm Nia, H. Salarzadeh Jenatabadi, P. M. Woi, E. Abouzari-Lotf, & Y. Alias, "The optimization of effective parameters for electrodeposition of reduced graphene oxide through Taguchi method to evaluate the charge transfer," Measurement (Lond), vol. 137, pp. 683–690, Apr. 2019.

[28] M. Liu, R. Liu, & W. Chen, "Graphene wrapped Cu2O nanocubes: Non-enzymatic electrochemical sensors for the detection of glucose and hydrogen peroxide with enhanced stability," Biosens Bioelectron, vol. 45, no. 1, pp. 206–212, Jul. 2013.